Case Studies in Nondestructive Testing and Evaluation 6 (2016) 63–69

Contents lists available at ScienceDirect

Case Studies in Nondestructive Testing and Evaluation

www.elsevier.com/locate/csndt

An innovative vehicle-mounted GPR technique for fast and efficient monitoring of tunnel lining structural conditions

Yuewen Zan [a,*], Zhilin Li [a], Guofeng Su [a], Xiyuan Zhang [b]

[a] State–Province Joint Engineering Laboratory of Spatial Information Technology for High-Speed Railway Safety, Southwest Jiaotong University, Chengdu 611756, China
[b] Xi'an Jiaotong University, Xi'an 710049, China

ARTICLE INFO

Article history:
Available online 14 October 2016

ABSTRACT

The health status of a railway tunnel should be regularly inspected during its service period to ensure safe operation. Ground-penetrating radar (GPR) has been used as a key technique for tunnel detection; however, so far, the measurements of GPR are only obtainable in contact mode. Such methods cannot meet the requirements of the operational tunnel disease census and regular inspections. Therefore, a new method—vehicle-mounted GPR with long-range detection—has been developed. It consists of six channels. The distance from its air-launched antenna to the tunnel lining is approximately 0.93 m–2.25 m. The scanning rate of each channel is 976 1/s. When the sampling point interval is 5 cm, the maximum speed can reach up to 175 km/h. With its speed and air-launched antenna, this system has a significant advantage over existing methods. That is, for an electrified railway, there is no need for power outages. Indeed, the proposed system will not interrupt normal railway operation. Running tests were carried out on the Baoji–Zhongwei and Xiangfan–Chongqing railway lines, and very good results were obtained.

1. Introduction

Regular inspections and health assessments are conducted for the repair and maintenance of tunnels. Railway tunnels, operating for a certain period of years, are aging and appear to be diseased, which is a worldwide problem. For example, in China, there presented the lining block-falling of tunnel vault for many times in 2001. The most significant accident occurred when a 30-m-long vault block suddenly collapsed and interrupted traffic for 10 days [1]. After the Taiwan earthquake of 1999, 57 tunnels were investigated, and 85.96% exhibited different degrees of disease [2]. According to a study of 302 operating highway tunnels in Hokkaido conducted by the highway tunnel branch of the Japanese Hokkaido Civil Engineers Association in 1986, there were diseases in 46.69% of the tunnels [3]. Undoubtedly, to eliminate these hazards in a timely fashion and to ensure operational safety, regular health inspections of tunnels are crucial.

Regular tunnel inspections are challenging. Nowadays, the traditional methods of GPR include a handheld antenna and hydraulic supporting antenna, which require power outages during maintenance times. The efficiency of both approaches is quite low because their antennas are close to the tunnel walls. Moreover, the antenna must go up and down when the drop post of the electrification catenary appears. As a result, the detecting speed is slow. Currently, there seems to be no traffic-interference-free nondestructive testing (NDT) method used to evaluate tunnel linings. Therefore, finding a fast

* Corresponding author.
E-mail address: dhxyzyw@home.swjtu.edu.cn (Y. Zan).

http://dx.doi.org/10.1016/j.csndt.2016.10.001

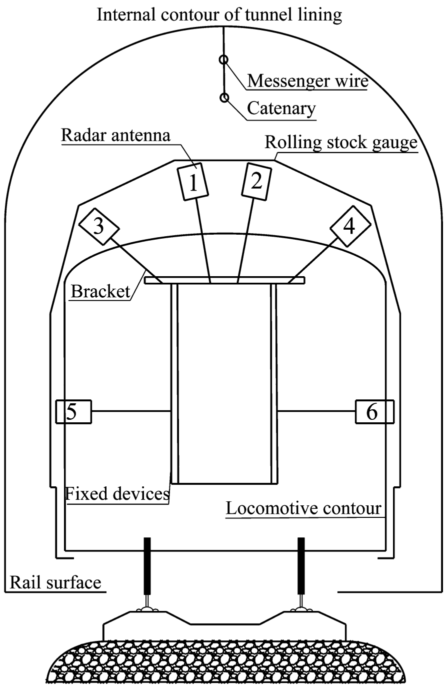

Fig. 1. Locations of the six antennas for vehicle-mounted GPR.

and nondestructive inspection method for tunnel health conditions has always been a concern in the field of the tunnel maintenance.

2. Design and method

2.1. Detection speed

In order to improve the detection speed, two problems need to be solved: the train must operate normally without a collision between the antenna and catenary, and the scanning rate of the GPR system should be high enough.

To solve the first problem, the GPR antenna must be mounted within the rolling stock gauge, and six sets of antennas should be fixed on the train. In China, for an electric single-track tunnel, the distance from the antennas to the tunnel wall is 93–133 cm (antenna 5 and antenna 6, in Fig. 1), and the distance from the antenna to the tunnel vault is 175–225 cm (antenna 1 and antenna 2). Therefore, the average distance from an air-launched antenna to the lining is 159 cm. Thus, a new detecting scheme that uses an air-launched antenna at a long distance from the tunnel wall was proposed.

The solution to the second problem is to increase the scanning rate of the GPR system. The scanning rate must meet the requirements of the designed testing speed. Assuming that the designed measuring-point spacing is 5 cm, the single-channel scanning rate for the GPR should be at least 444 1/s if we want to test at a speed of 80 km/h. In reality, the scanning rate of each channel of this system is 976 1/s, so the highest test speed of 175 km/h can be reached.

2.2. Detection efficiency

Improving the detection efficiency requires the use of a multichannel GPR system. Therefore, a detecting system with six channels and six measuring lines was arranged (Fig. 1). This system can detect a tunnel with a full-section mode.

2.3. 300-MHz air-launched antenna

Because the ground-coupled antenna suffers from a “blind zone” effect, shallow anomalies such as defects within the lining will be difficult to distinguish [4,5]. The depth of the blind zone extends from the surface to a depth of 1.5 times the wavelength [6], as shown in Fig. 2. The range of the blind zone is almost equal to the near-field range. In this region, the direct-coupled wave signal is too strong to expose to both the reflected wave from the lining surface and the reflected signal from the surface defect.

We developed a 300-MHz air-launched antenna whose wavelength in the air is 100 cm. A distance of 1.5 times the wavelength in the air is close to the average distance between the antenna and the tunnel wall (159 cm). This is the

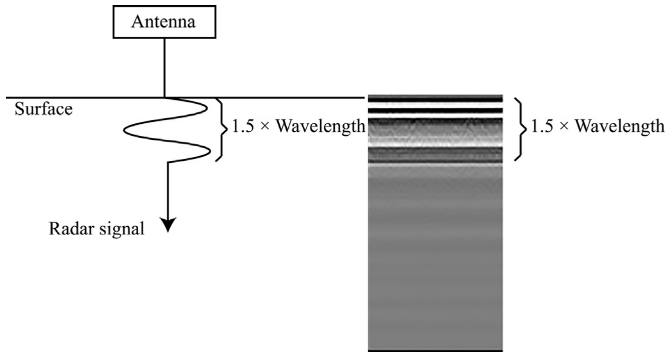

Fig. 2. Schematic diagram of blind zone [6].

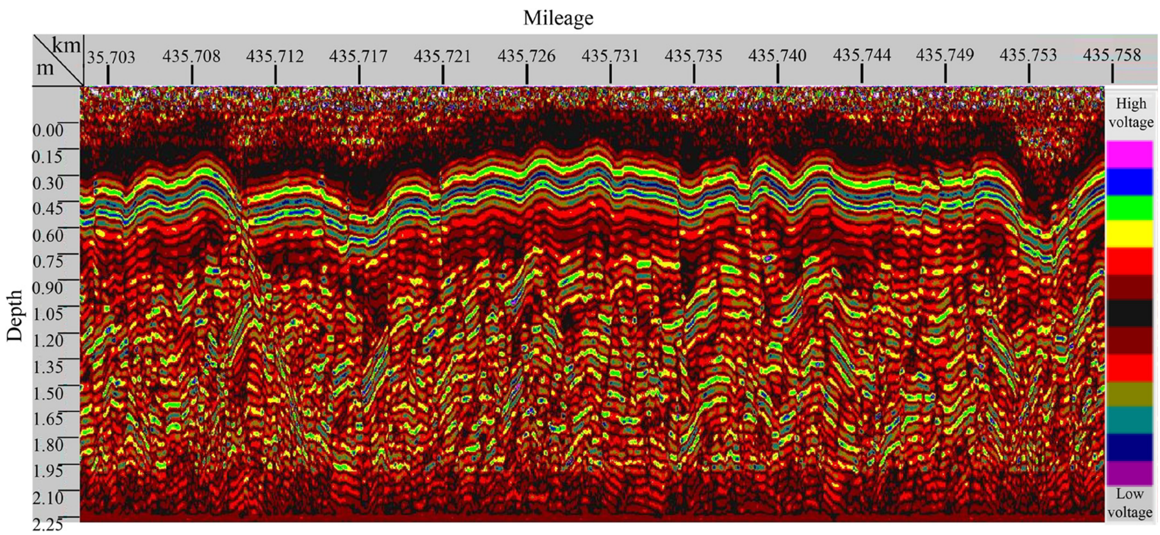

Fig. 3. Radar image for shotcrete lining with rough surface.

distance that makes the air-launched antenna operational in the far-field range. Thus, we can see the surface state and geometry of the lining, as shown in Fig. 3.

Fig. 3 shows a radar image of the shotcrete lining of Yanshan tunnel. With good tunnel surrounding rock, only the spray anchor bracing was constructed after blasting. The radar image can reflect the geometry of the spray anchor lining. Therefore, for this detection method, by comparing radar images over the years, deformations in the tunnel lining can be found.

3. System and parameters

The vehicle-mounted GPR system for tunnel detection consists of six channels, a positioning system, and a data processing system. Photographs of the system are shown in Fig. 4.

Six-channel GPR system: The pulse repetition frequency of each channel is 500 kHz, the antenna center frequency is 300 MHz, and the scanning rate of each channel is 976 1/s. Each scan has 512 points, and the time window is designed with 60 ns/screen. The receiver's maximum noise is 0.75 mV, and the A/D converter has 16 bits. The size of the antenna is 800 mm (length), 200 mm (width), and 250 mm (height).

Positioning technique: We adopted a positioning method combined with distance measurement and GIS correction. Namely, using GPS and GIS systems, we automatically obtained the mileage outside the tunnel. The mileage sensor measures the distance inside the tunnel. This allows the vehicle-mounted GPR system to detect the entire line at once, which is continuous and fully automated.

Data processing technique: The post-processing software can process six-channel data simultaneously with a fast processing speed and small storage capacity without any transition files. The multichannel processing software can display the six channels of data, or any channel data. The data processing procedure is shown in Fig. 5.

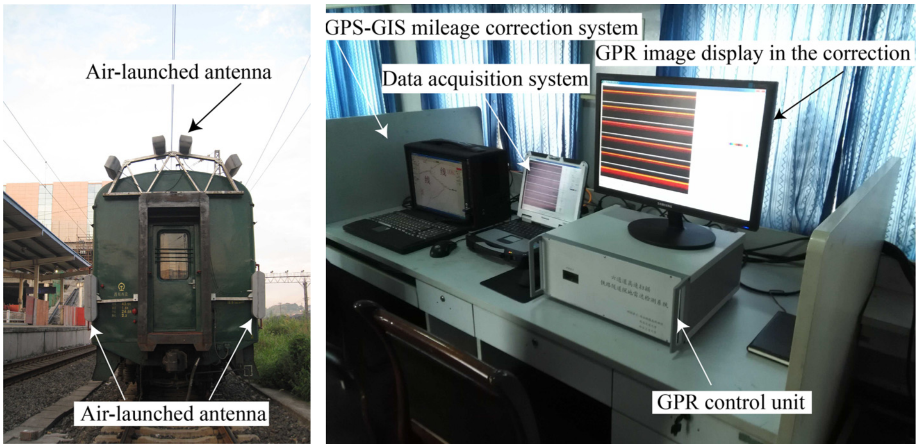

Fig. 4. Vehicle-mounted GPR system.

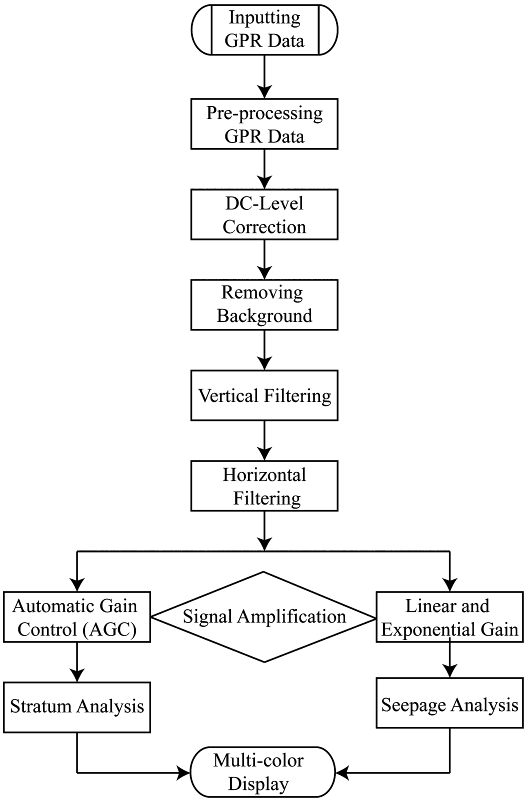

Fig. 5. Flowchart of data processing.

4. Experimental results

The railway vehicle-mounted GPR system was tested in electrified railway tunnels on the Baoji–Zhongwei line and the Xiangfan–Chongqing line in 2013. We obtained a significant amount of observed data, which has been analyzed and verified.

Fig. 6 shows that the reinforcing section (with a steel arch and ejector anchor) can be identified, and that the length of the steel arch reinforcement section and steel arch interval can be accurately determined. A section of the lining appears disconnected and convex. In addition, crescent-shaped reflections are visible. It was verified afterward that Yanjiashan tunnel, built in July 1993, had some diseases after operation. The tunnel has serious longitudinal and transverse cracks with a 25 mm–40 mm cracking width and 50 mm–70 mm convex height, as well as local dropping block. From June 2003 to July 2005, the railway administration department conducted bolt-grouting reinforcement along a 140-m-length arch of the tunnel that contained diseases, setting a P34 at each meter of the steel arch.

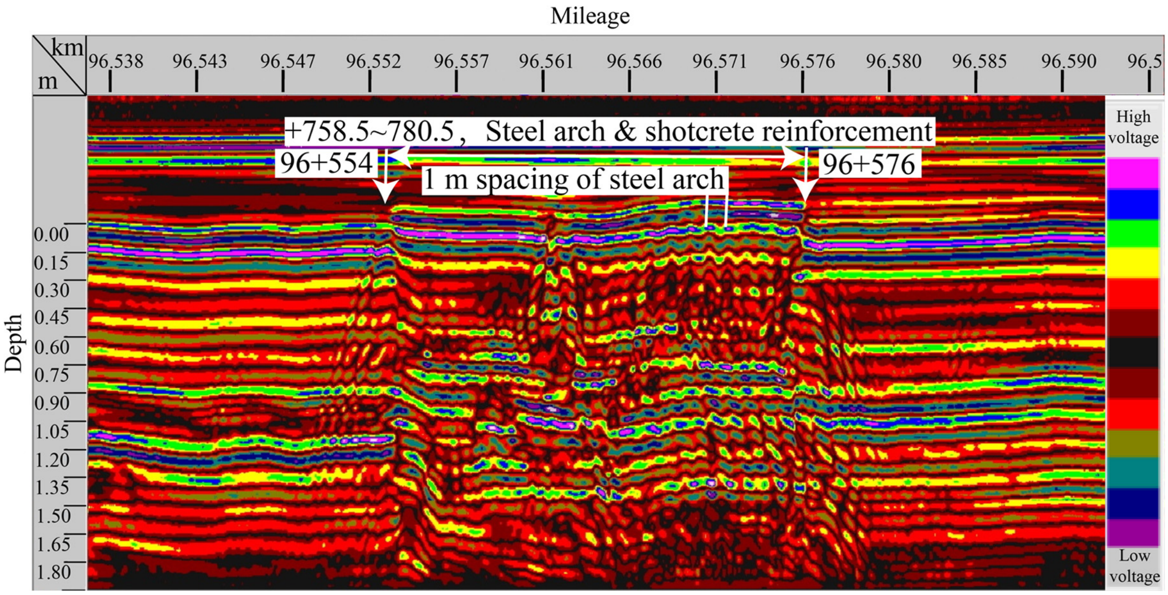

Fig. 6. Radar image of arch top of Yanjiashan tunnel from k96 + 545 to k96 + 578.

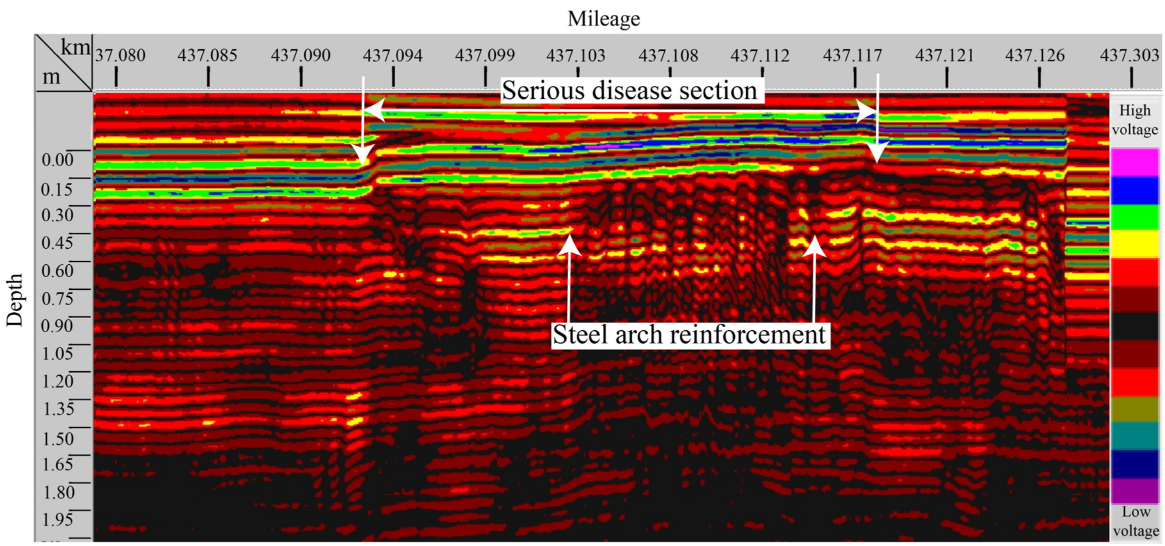

Fig. 7. Radar image of significant disease in left vault of Daping tunnel.

Fig. 7 shows a radar image of the vault lining of the Daping tunnel in 2013. From K437 + 093.5 to K437 + 118.5, diseases were significant. Repairs were conducted in 2010 by chiseling a groove inside the arch lining at each meter, inserting a permanent rail arch, and filling it with C20 concrete. The length of the serious defect section and the interval of the steel arch in the radar image are consistent with the design [7].

Fig. 8 shows a radar image of the arch top in the Qingliangshan tunnel on the Baoji–Zhongwei railway line in 2012. The image shows the section from K102 + 137 to K102 + 144, where a large deformation occurred. This area was reinforced with a steel arch and spray anchor grouting. It can be seen from the radar image that the deformation of the surrounding rock appears to have a curved contour. After this was confirmed, a collapse and large deformation occurred during the construction process, and reinforcement was required.

Part of the radar image that shows water seepage in the vault of Guanyinxia tunnel is shown in Fig. 9. The strong reflecting image on the lining surface indicates water seepage.

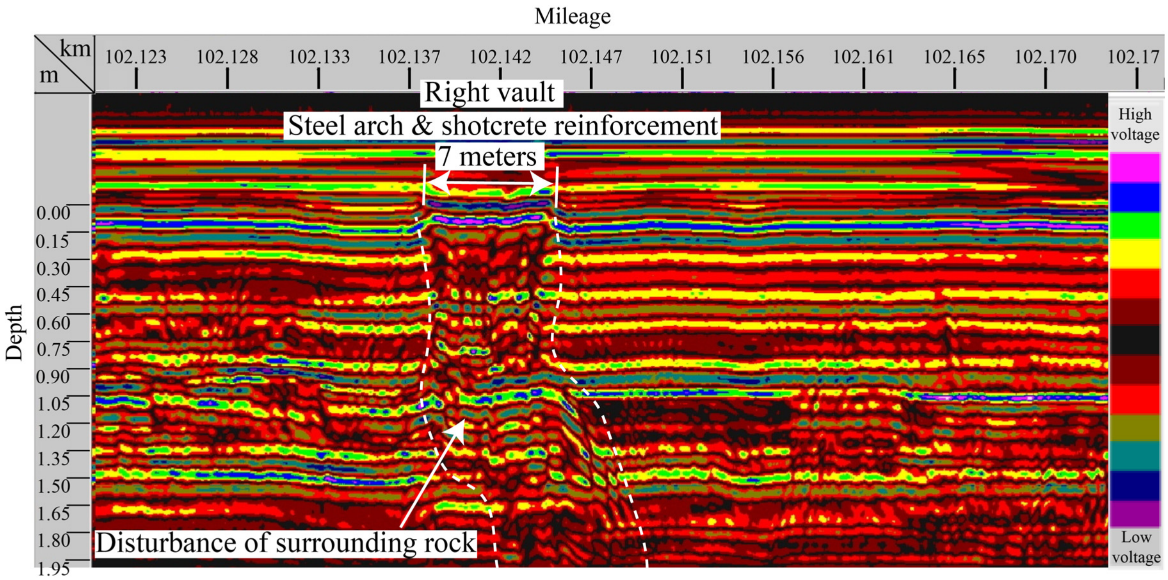

Fig. 8. Radar image of arch top of Qingliangshan tunnel from K102 + 137 to K102 + 144.

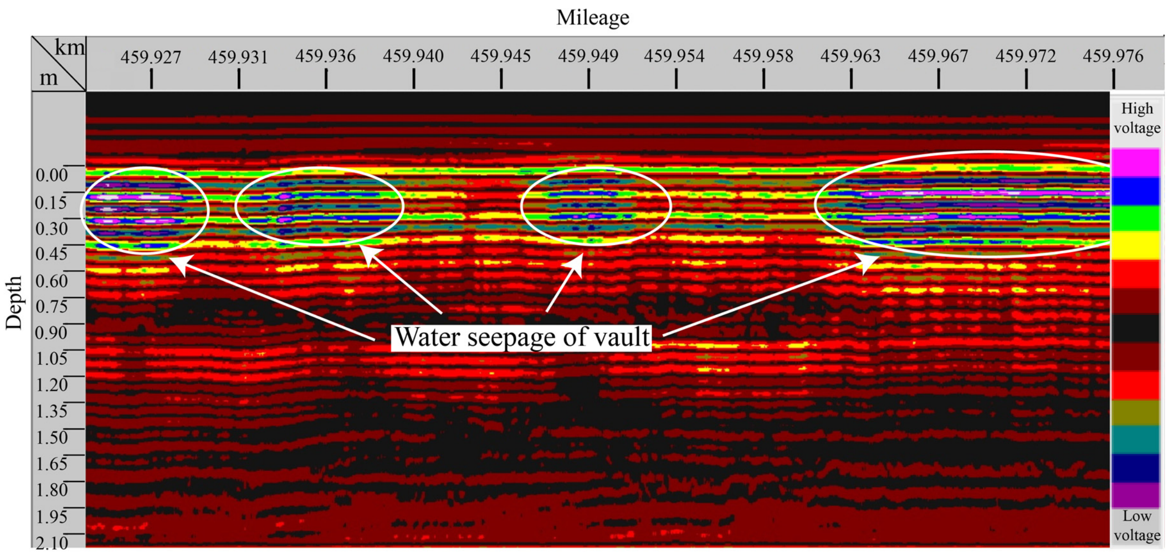

Fig. 9. Radar image for water seepage of vault in Guanyinxia tunnel.

5. Discussion and conclusion

Compared to ordinary GPR, for air-launched antennas of vehicle-mounted GPRs working in the far field [8], direct waves are separated from reflection waves of the lining surface. Then, areas with damaged lining can be clearly seen.

Instead of using the method discussed by A. Wimsatt et al. (2013), our proposed data analysis method adopts an analytical imaging method. Using the properties of the image, some information can be easily identified: integrity and deformation, disturbance of the surrounding rock, steel arches inside the lining, and the flatness of the lining surface.

The vehicle-mounted GPR system, which can detect an entire railway line in a short amount of time, provides a fast, interference-free method for periodic inspections and health assessments of existing tunnels.

Acknowledgements

It is gratefully acknowledged that the work presented in this paper has been sponsored by the MOE's Program for Changjiang Scholars and Innovative Research Team (IRT13092) and the "2011 Collaborative Innovative Research Center."

References

[1] Wu JB, Zhang DL, Wang MS. Operational railway tunnel disease status and evaluation. China Saf Sci 2003;13(6):49–52.
[2] Wang WL, Wang TT, Su JJ, et al. Assessment of damage in mountain tunnels due to the Taiwan Chi-Chi earthquake. Tunn Undergr Space Technol 2001;16(3):133–50.
[3] Akira I, Shigero I. Road tunnel in Japan: deterioration and counter measures. Tunn Undergr Space Technol 1996;11(3):305–9.
[4] Grant JA, Campbell BA, Schutz AE. A rover deployed ground penetrating radar on Mars. In: Clifford S, George J, Stoker C, editors. Proceedings of the IEEE conference on the geophysical detection of subsurface water on Mars. LPI Contrib, vol. 1095. Houston, Tex, USA: Lunar and Planet. Inst.; 2001. p. 41–2.
[5] Ernenwein EG. Imaging in the ground-penetrating radar near-field zone: a case study from New Mexico, USA. Archaeol Prospect 2006;13(2):154–6.
[6] Maurer JA IV. Local-scale snow accumulation variability on the Greenland ice sheet from ground-penetrating radar (GPR). Master dissertation. Colorado, USA: Colorado University; 2006.
[7] Tian H. Study on the comprehensive treatment of defects in K437 + 320 DaPing tunnel on Xiang Yu railway. Railw Constr Technol 2011;8:42–3.
[8] Diamanti N, Annan P, Redman D. Quantifying GPR responses. In: Proceedings of 14th international conference on ground penetrating radar. 2012. p. 237–42.